International Journal of Computer Science, Communication & Information Technology (CSCIT)
Vol.7 pp. 22-29

Hybrid color MRI image compression by level set method and quincunx wavelet

Imane Haouam#1, Mohammed Beladgham*2,, Abdelmalik Taleb-Ahmed*3

[1,2]*Department of Electrical Engineering,*

[1,2]*TIT Laboratory, Tahri Mohammed University of Bechar, Bechar, Algeria*

[3]*Laboratoire IEMN DOAE. UMR CNRS 852, Valenciennes France*

1imahaouam@gmail.com

2beladgham.tlm@gmail.com

3Abdelmalik.Taleb-Ahmed@univ-valenciennes.fr

Abstract— **In recent years, researchers have increasingly targeted the development of hybrid systems to improve the quality of the compressed image. Hybrid methods are combinations of several techniques that take into account the advantages and disadvantages of it, in order to obtain a better image quality with a high compression ratio in a minimal calculation time. In this article, we are interested in geometric active contours techniques using the level-set method and the quincunx wavelet , so we proposed an hybrid algorithm for color medical image compression based on the level set method and the quincunx wavelet transform coupled with the set partitioning in hierarchical trees (SPIHT) algorithm. Experimental results show that the proposed algorithm gives better results compared to various methods, where it provides very important PSNR and MSSIM values.**

Keywords— **Color Medical image, Compression, level set, quincunx wavelet, SPIHT, PSNR**

I. INTRODUCTION

The compression of medical images becomes a necessity to reduce their size, in order to ensure their archiving and facilitate their transmission. Currently hybrid methods acquired a huge popularity by aiming to match the advantages of each one, in order to obtain a powerful method with a high compression ratio, by giving a better image quality. It should be noted that magnetic resonance imaging has quickly become a critical study technique for the skull and brain.

The segmentation of the medical image gives an accurate analysis of the pathology while basing on the essential part of the image that contains the disease for a better diagnosis. Among the methods that have been proven in medical imaging segmentation, active contours, and in particular those based on "region", remain among the most adapted because they offer the possibility of taking into account a statistical aspect of the target region and therefore of integrate the specificities of the physical principle of acquisition into the segmentation process.

The segmentation by active contours aims to partition an image into different regions of interest, by means of an iterative process that allows an initiative curve to evolve towards the regions of interest, this deformation of contour is moved by image driven forces. Various medical image segmentation methods have been explored and widely presented in the literature [1]-[4]

This article aims to develop a method for better color medical image compression using quincunx wavelets which are better adapted to the image representation and was the subject of various research

The quincunx wavelet offers an optimal representation for image geometric. This structure of decomposition allows the construction of a non separable transform. Non separable wavelets, by contrast, offer more freedom and can be better tuned to the characteristics of images. Their less attractive side is that they require more computations. The quincunx wavelets are especially interesting because they are nearly isotropic. In contrast with the separable case, there is a single wavelet and the scale reduction is more progressive: one factor instead of 2[5]

Including to these two methods and their advantages, in this work we propose the quincunx algorithm coupled with the level set method for MRI color image compression. We enhance the image compression by our algorithm, by a comparison of the PSNR, MSSIM and MSE results obtained with the existing techniques

ISSN 1737-930X

II. THE METHODS.

A. *Level set method*

A large number of technique and methods have been proposed and used [6]-[8]

It was first introduced by Osher and Sethian [9] who proposed an effective implicit representation for evolving curves and surfaces, it allows for automatic change of topology, such as merging and breaking, and the calculations are made on a fixed rectangular grid, where The basic idea is to represent the curves or surfaces as the zero level set of a higher dimensional hyper-surface. The level set method proposed in [10] is used to solve the minimization problem of [11]

In the level set method, an interface C is represented implicitly as a level set of a function φ, called level set function, of higher dimension. The geometric characteristics and the motion of the front are computed with this level set function. The interface is now represented implicitly as the zero-th level set (or contour) of this scalar function. Specifically, given a closed curve C, the function is zero if the pixel lies on the curve itself, otherwise, it is the signed minimum distance from the pixel to the curve.

This method makes it possible to evolve a closed parametric curve C (p) according to an equation of the type $\frac{\partial c}{\partial t} = FN$ [12]:

Where t is time, F is the rate of evolution and N is the unit normal to the curve. Each point of the curve C evaluates in the normal direction to the curve with a speed F as shown in Fig.1

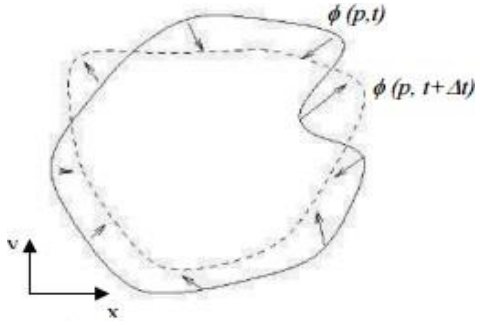

Fig. 1 The curve C evolved according to $\frac{\partial c}{\partial t} = FN$

Level set function $\phi(x, y)$, considering that $\phi(x, y) > 0$ if the point (x, y) inside c, $\phi(x, y) < 0$ if the point (x, y) is outside c $\phi(x, y) = 0$ if the point (x, y) is on c. Thus, the energy functional F(c1, c2, C) can be reformulated in terms of the level set function (x, y) as follows [13]:

$$F(c1, c2, \phi) = \lambda_1 \int_{\Omega} / I(x, y) - c1 /^2 H\varepsilon(\phi(x, y))dxdy + \lambda_2 \int_{\Omega} / I(x, y) - c2 /^2 (1 - H\varepsilon((\phi(x, y)))dxdy + \mu \int_{\Omega} \delta(\phi(x, y)) / \nabla\phi(x, y) / dxdy \quad (1)$$

Where H(Z) and $\delta\varepsilon(z)$ are, respectively, the regularized approximation of Heaviside function H and delta function δ as follows :

$$H(Z) = \begin{cases} 1 \vec{\ } if \bar{\ } z \geq 0 \\ 0 \bar{\ } if \bar{\ } z \prec 0 \end{cases} \qquad \delta(z) = \frac{d}{dz} H(z) \quad (2)$$

Using the Euler-Lagrange equations to solve the minimization problem of (1), the level set function (x, y) can be updated by the following gradient descent method:

$$\frac{\partial \phi}{\partial t} = \delta\varepsilon(\phi)\left[\mu div(\frac{\nabla\phi}{|\nabla\phi|}) - \lambda_1 (I - c1)^2 + \lambda_2 (I - c2)^2 \right] \quad (3)$$

Where c1 and c2 can be expressed, respectively, as follows:

$$c1(\phi) = \frac{\int_{\Omega} I(x, y) H\varepsilon(\phi(x, y))dxdy}{\int_{\Omega} H\varepsilon(\phi(x, y))dxdy}$$

$$c2(\phi) = \frac{\int_{\Omega} I(x, y)(1 - H\varepsilon(\phi(x, y)))dxdy}{\int_{\Omega} (1 - H\varepsilon(\phi(x, y)))dxdy} \quad (4)$$

This technique not only provides more accurate numerical implementations but also handle topological change very easily. The main advantage of this method is the ability to automatically manage the change in topology of the evolving curve. The curve C can be divided into two or three curves; conversely several curves can merge and become a single curve

In image processing the level set method is most frequently used as a segmentation tool through propagation of a contour by using the properties of the image

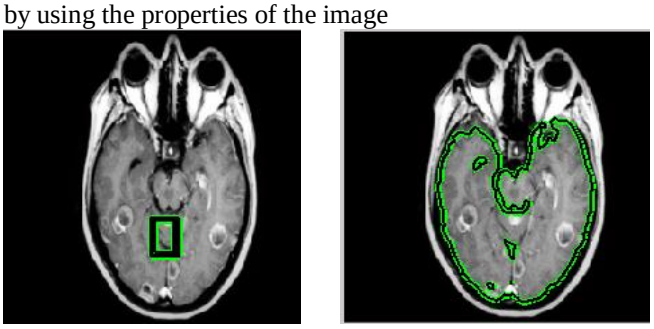

(a) (b)

ISSN 1737-930X

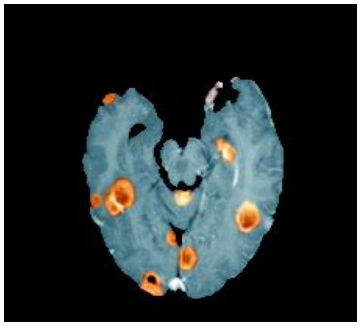

(c)

Fig.2 level set segmentation steps (a) Curve initialization, (b) level set segmentation, (c) foreground extraction

B. Quincunx wavelet

The separable dyadic analysis require three families of wavelets, which is sometimes regarded as a disadvantage, in addition the factor of addition between two successive scales is 4 which may seem high. It is possible to solve these two problems, but at the cost of the loss of filter separability and therefore a slightly higher computational complexity. An analysis has been particularly well studied to find a practical application, known as "quincunx" [14]. Quincunx decomposition results in fewer subbands than most other wavelet decompositions, a feature that may lead to reconstructed images with slightly lower visual quality. The method is not used much in practice, but [15] presents results that suggest that quincunx decomposition performs extremely well and may be the best performer in many practical situations. Fig. 3 illustrates this type of decomposition. [16]

We notice that the dilation factor is not more than 2 between two successive resolutions, and that only one wavelet family is necessary [17, 18]. In this case the

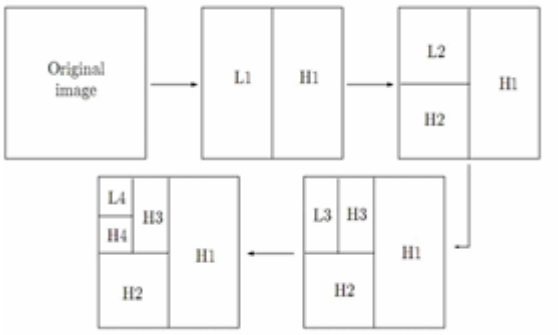

Fig. 3. Quincunx wavelet decomposition

In this case the Dilatation matrice will be :

$$M=\begin{bmatrix}1 & 1\\ 1 & -1\end{bmatrix}$$

The Grid transformation (lattice) is done according to $y_{i+1}[n]$ the following diagram:

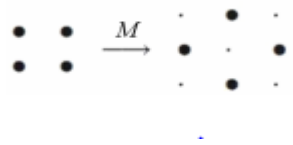

This matrix generates a quincunx lattice in 2D. The column vectors of this matrix form a basis to this lattice. The volume of the unit cell associated equals 2. The same lattice Fig. 4 is also emanating from the matrix below [14]

$$M'=\begin{bmatrix}1 & -1\\ 1 & 1\end{bmatrix}$$

It is noticed that the dilatation step is $\sqrt{2}$ on each direction and the geometry of the grid obtained justifies the name given to this multiresolution analysis

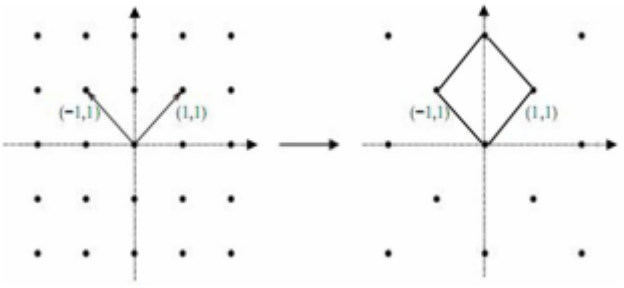

(a) (b)

Fig. 4. Examples of a lattice quincunx and unit cell (a) Lattice quincunx (b) Unit cell

1) Quincunx Sampling and Filter

First, we recall some basic results on quincunx sampling and perfect reconstruction filterbanks [19, 20]. The quincunx sampling lattice is shown in Fig. 4. Let $x[\vec{n}]$ with $\vec{n}=(n_1,n_2) \in Z^2$ denote the discrete signal on the initial grid. The two-dimensional (2-D) z-transform of $x[\vec{n}]$ is denoted by:

$$X(\vec{z})=\sum_{\vec{n}\in Z^2} x[\vec{n}]\vec{z}^{-\vec{n}} \quad \text{, where} \quad \vec{z}^{\vec{n}}=\vec{z}^{n_1}\vec{z}^{n_2} \tag{5}$$

The continuous 2-D Fourier transform is then given by

$$X(e^{j\varpi})=\sum_{\vec{n}\in Z^2} x[\vec{n}]e^{-j(\vec{w},\vec{n})} \quad \text{with} \quad \vec{w}=(w_1,w_2) \tag{6}$$

and finally, the discret 2-D Fourier transform for $x[\vec{n}]$ given on an N x N grid (n1, n2= 0,1,…,N-1) by

ISSN 1737-930X

$$X\left(\vec{k}\right)=\sum_{\vec{n}\in z^2} x\left[\vec{n}\right]e^{-j2\pi(\vec{k},\vec{n})/N},$$

With (k1,k2=0,1,…, N-1)

Now, we write the quincunx sampled version of x[$\vec{n}$] as:

$$\left[x\right]_{\downarrow M}\left[\vec{n}\right]=x\left[M\vec{n}\right] \quad \text{where} \quad M=\begin{pmatrix}1 & 1\\ 1 & -1\end{pmatrix} \tag{7}$$

Our down-sampling matrix M is such that $M^2 = 2$ I. where I is identity matrix.

The Fourier domain version of (2) is

$$\left[x\right]_{\downarrow M}\left[\vec{n}\right]=\leftrightarrow\frac{1}{2}\left[X\left(e^{jM^{-T}\vec{\omega}}\right)+X\left(e^{j\left(M^{-T}\overrightarrow{\omega+\pi}\right)}\right)\right] \tag{8}$$

Where $\vec{\pi}$ =(π , π) .

The up-sampling is defined by

$$\left[x\right]_{\uparrow M}\left[\vec{n}\right]=\begin{cases}x\left[M^{-1}\vec{n}\right], when n_1+n_2\\ 0 elsewhere\end{cases} \tag{9}$$

and its effect in the Fourier domain is as follows:

$$\left[x\right]_{\uparrow M}\left[\vec{n}\right]=\leftrightarrow X\left(e^{jM^{T}\vec{\omega}}\right) \tag{10}$$

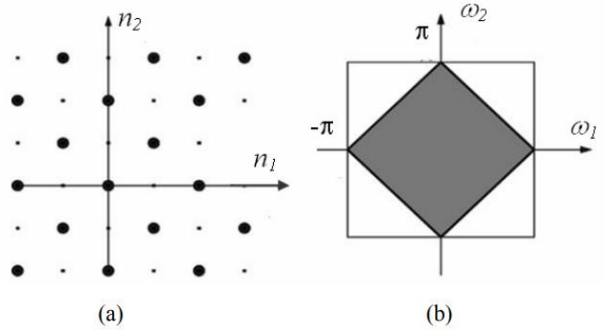

Fig. 5. (a) Quincunx lattice; (b) the corresponding Nyquist area in the frequency domain

If we now chain the down-sampling and up-sampling operators, we get

$$\left[x\right]_{\downarrow M\uparrow M}\left[\vec{n}\right]=\begin{cases}x\left[\vec{n}\right], when n_1+n_2 is even\\ 0 elsewhere\end{cases} \tag{11}$$

$$\left[x\right]_{\downarrow M\uparrow M}\left[\vec{n}\right]=\frac{1}{2}\left[X\left(e^{j\vec{\omega}}\right)+X\left(e^{j(\vec{\omega}+\vec{\pi})}\right)\right] \tag{12}$$

Since quincunx sampling reduces the number of image samples by a factor of two, the corresponding reconstruction filterbank has two channels Fig. 6. The low-pass filter $\tilde{H}$ reduces the resolution by a factor of $\sqrt{2}$; the wavelet coefficients correspond to the output of the high-pass filter $\tilde{G}$ [18]-[20].

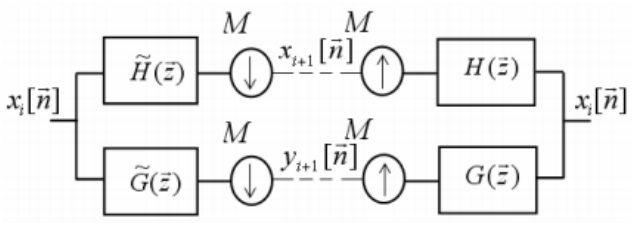

Fig. 6. Perfect reconstruction filter bank on a quincunx lattice

2) Fractional Quincunx Filters

As starting point for our construction, we introduce a new 1-D family of orthogonal filters

$$H_a(\omega)=\frac{\sqrt{2}(2+2\cos\omega)^{\frac{a}{2}}}{\sqrt{(2+2\cos\omega)^a+(2-2\cos\omega)^a}} \tag{13}$$

Which is indexed by the continuously-varying order parameter α.

Applying the diamond McClellan transform to the filter above is straightforward; it amounts to replacing cos ω by 1 2 (1/ 2)(cos $\omega_1+\cos\omega_2$) in (13). Thus, our quincunx refinement filter is given by

$$H_a(e^{j\omega})=\frac{\sqrt{2}(2+\cos\omega_1+\cos\omega_2)^{\frac{a}{2}}}{\sqrt{(2+\cos\omega_1+\cos\omega_2)^a+(2-\cos\omega_1-\cos\omega_2)^a}} \tag{14}$$

This filter is guaranteed to be orthogonal because the McClellan transform has the property of preserving biorthogonality. Also, by construction, the α th order zero at ω =π gets mapped into a corresponding zero at $(\omega_1,\omega_2)=(\pi,\pi)$; this is precisely the condition that is required to get a 2-D wavelet transform of orderα . Also, note the isotropic behavior and the flatness of $H_a(e^{j\omega})$ around the origin; i.e, $H_a(e^{j\omega})/\sqrt{2}=1+O(\|\vec{\omega}\|^a)$ for $\vec{\omega}\to 0$. The orthogonal wavelet filter is obtained by modulation

$$G_a(\vec{z})=z_1H_a(-\vec{z}^{-1}) \tag{15}$$

The corresponding orthogonal scaling function is defined implicitly as the solution of the quincunx two-scale relation

$$\varphi_a(\vec{x})=\sqrt{2}\sum_{\vec{n}\in z^2}h_a\left[\vec{n}\right]\varphi_a\left(M\vec{x}-\vec{n}\right) \tag{16}$$

Since the refinement filter is orthogonal with respect to the quincunx lattice, it follows that $\varphi_a(\vec{x})\in L_2\left(R^2\right)$ and that it is orthogonal to its integer translates. Moreover, for α >0 , it will satisfy the partition of unity condition, which comes as a direct consequence of the vanishing of the filter at

ISSN 1737-930X

$(\omega_1, \omega_2) = (\pi, \pi)$Thus, we have the guarantee that our scheme will yield orthogonal wavelet bases of $L_2(R^2)$. The underlying orthogonal quincunx wavelet is simply

$$\psi_a(\vec{x}) = \sqrt{2} \sum_{\vec{n} \in z^2} g_a[\vec{n}] \varphi_a(M\vec{x} - \vec{n}) \quad (17)$$

C. SPHT Coding scheme

SPIHT algorithm is an improved version of EZW algorithm proposed by A. Said and Pearlman [18] SPIHT performs a recursive partitioning of the tree in order to determine the position of the significant coefficients in the progeny of the considered coefficient

The success of SPIHT is due to the organisation of wavelet coefficients into the spatial orientation trees.

The following sets of coordinates are used to present the new coding method:

O (i, j) : set of coordinates of all offspring of node (i, j);

D (i, j) : set of coordinates of all descendants of the node (i, j);

H: set of coordinates of all spatial orientation tree roots (nodes in the highest pyramid level);

L (i, j) = D(i, j) - O(i, j).

In a practical implementation the significance information is stored in three ordered lists, called list of insignificant sets (LIS), list of insignificant pixels (LIP), and list of significant pixels (LSP). In all lists each entry is identified by a coordinate (i, j), which in the LIP and LSP represents individual pixels, and in the LIS represents either the set D (i, j) or L (i, j).

The first idea is always the same: if there is a coefficient in the highest level of transform in a particular subband considered insignificant against a particular threshold, it is very probable that its descendants in lower levels will be insignificant too, so we can code quite a large group of coefficients with one symbol. Fig.7 shows how a spatial orientation tree is defined in a pyramid constructed with recursive four subbands splitting. The coefficients are ordered in hierarchies [21]

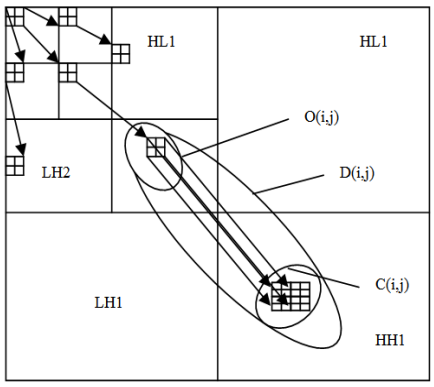

Fig. 7 Parent-child relationship

D. Quality evaluation parameter

3) The peak signal to noise ratio (PSNR).

The peak signal to noise ratio (PSNR) used to measure the quality of reconstruction in image compression. It refers to the ratio between signal and reconstruction error variance in Decibel scale. It can be represented as [22]:

$$MSE = \frac{1}{M\,x\,N} \sum_{1=1}^{i=M} \sum_{j=1}^{j=N} \left(I(i,j) - \hat{I}(i,j)\right)^2 \quad (18)$$

Where

MSE: mean squar error between two images

Mean Square Error (MSE) which requires two MxN grayscale images I and $\hat{I}$ where one of the images is considered as a compression of the other

The PSNR is defined as:

$$PSNR = 10 \log_{10} \left(\frac{(Dynamics \quad of \quad image)^2}{MSE} \right) \quad (19)$$

4) The Structural Similarity Index(SSIM).

This parameter compares the similarity the brightness, contrast and structure between each pair of vectors, the structural similarity index between two signals x and y is given by the following expression [23,24]:

$$SSIM(x,y) = l(x,y).c(x,y).s(x,y) \quad (20)$$

The MSSIM is used to measure the quality of the local image, which provides more information on the degradation of image quality, which is useful in medical imaging applications. It values exhibit greater consistency with the visual quality.

$$MSSIM(I,\hat{I}) = \frac{1}{M} \sum_{i=1}^{M} SSIM(I_i, \hat{I}_i) \quad (21)$$

Where

I and Î are respectively the reference and degraded images, I_i and $\hat{I}_i$ are the contents of images at the i-th local window.

M: the total number of local windows in image.

Finally the quality measurement can provide a spatial map of the local image quality, which provides more information on the image quality degradation, which is useful in medical imaging applications.

III. RESULTS AND DISCUSSION

The aim of our work lies in the possibility of reducing the rates, for which the image quality remains acceptable, which we are interested in hybrid compression methods based on activ contour segmentation and 2D wavelet transforms because of their interesting properties, applied to medical images. For this reasons the PSNR evaluation parameters and the MSSIM similarity index are used to estimate and judge the quality of the compressed image.

In order to verify the efficiency of our hybrid algorithm, we applied, (level set +CDF 9/7 (lifting scheme) + SPIHT)

ISSN 1737-930X

and (level set +quincunx + SPIHT) on color MRI medical images of size 512x512 encoded by 8 bits per pixel. This image is taken from the GE Medical System database [25].

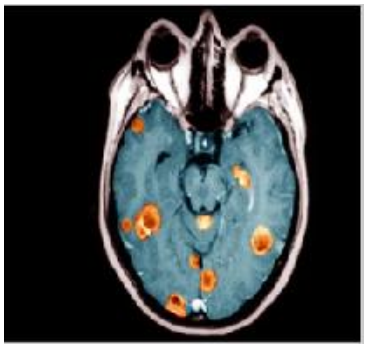

Fig. 8 MRI brain original image

Fig.9 shown below illustrates the steps of the compressed image (region of interest image) by the quincunx wavelet

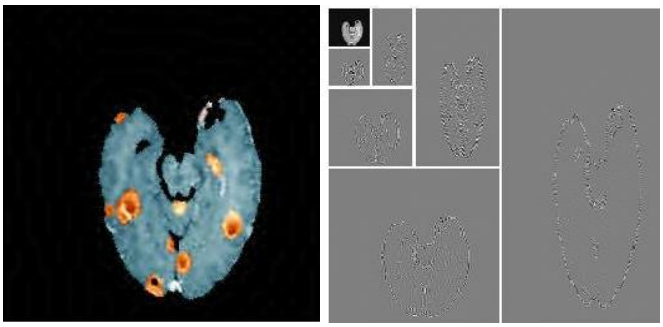

(a) (b)

Fig. 9 image compression (a) the region of interest (b) quincunx wavelet decomposition

The compressed image quality for different bit-rate values (number of bits per pixel) by the proposed algorithm is presented in the Fig .10

From the results of the PSNR, MSSIM and MSE values obtained, we note that from 0.5bpp, the reconstructed image becomes almost perfect.

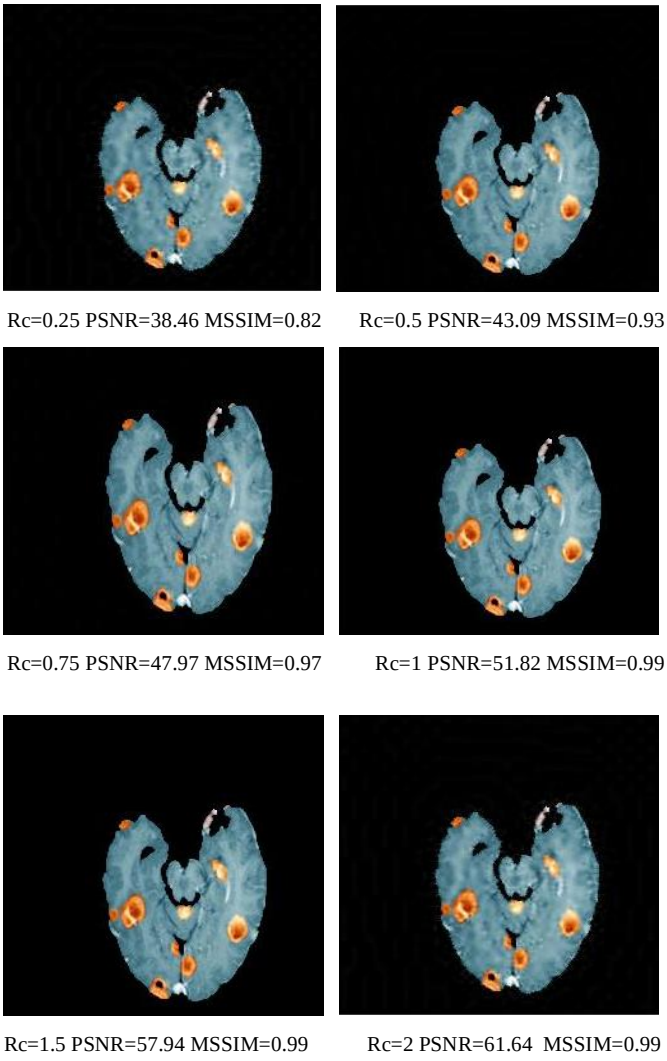

Rc=0.25 PSNR=38.46 MSSIM=0.82 Rc=0.5 PSNR=43.09 MSSIM=0.93

Rc=0.75 PSNR=47.97 MSSIM=0.97 Rc=1 PSNR=51.82 MSSIM=0.99

Rc=1.5 PSNR=57.94 MSSIM=0.99 Rc=2 PSNR=61.64 MSSIM=0.99

Fig..10 Compressing of an MRI brain image with level set coupled with quincunx wavelet and SPIHT coding

To ensure the performance of our proposed method, we compared between these different types of transform CDF9/7 (Lifting scheme)) coupled with level set method and SPIHT coding and CDF9/7 (Lifting scheme)) coupled with SPIHT coding without applied the level set segmentation applied to the same medical image. The table (1) and (2) given bellow represent these results

ISSN 1737-930X

TABLE I
PSNR AND MSSIM VARIATION USING DIFFERENT METHODS PROPOSED

Typed'image	RC (bpp)	Level set + quincunx + SPIHT			Level set + CDF9/7 (lifting) + SPIHT		
		PSNR	MSSIM	MSE	PSNR	MSSIM	MSE
IRM	0.25	38.46	0.82	9.27	36.12	0.47	16.03
	0.5	43.09	0.93	3.2	39.71	0.62	7.01
	0.75	47.97	0.97	1.04	44.19	0.79	2.5
	1	51.82	0.99	0.43	49.19	0.93	0.79
	1.5	57.94	0.99	0.11	57.77	0,99	0.11
	2	61.64	0.99	0.05	61.43	0.99	0.05

TABLE III
PSNR AND MSSIM VARIATION USING DIFFERENT METHODS PROPOSED

RC (bpp)	Quincunx +SPIHT			CDF9/7 (lifting)+ SPIHT		
	PSNR	MSSIM	MSE	PSNR	MSSIM	MSE
0.25	38.98	0.91	8.23	36.35	0.64	15.22
0.5	44.33	0.96	2.4	41.51	0.79	4.63
0.75	47.91	0.98	1.06	45.88	0.94	1.7
1	50.75	0.99	0.56	48.15	0.96	1.01
1.5	54.12	0.99	0.26	53.04	0.99	0.33
2	56.45	0.99	0.16	55.80	0.99	0.18

Comparing the different values of PSNR,MSSIM, and MSE we ensure the efficiency of our algorithm in terms of compressed image quality for the low bit-rate

The fig.11 shown bellow, represent the results of the comparison obtained after application of different algorithms applied on an MRI brain, given by the PSNR curve

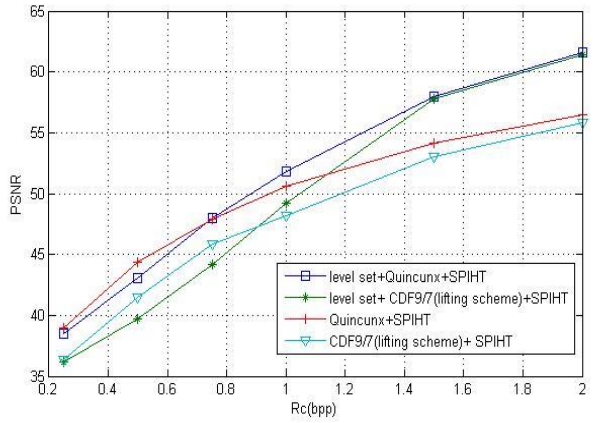

Fig. 11 PSNR variation using different proposed methods

According to the different results obtained for the several application of our hybrid method on color MRI medical image, we ensure that our proposed algorithm gives better quality and it is an efficient method compared with other technique, more precisely when compressed the region of interest image after applying the level set segmentation with quincunx algorithm coupled with SPIHT coding, which gives a better performance and image quality.

IV. CONCLUSIONS

The work in this paper is to enhance medical images quality after the compression step.

We used an hybrid method composed of the level set method and the quincunx wavelet transform applied on MRI color medical image. We compared the founding results with the level set coupled with CDF9/7 lifting algorithm and SPIHT, we notice that the proposed algorithm gives better results than the other compression technique for the MRI color image. Generally the results obtained are very satisfactory in terms of compression ratio and compressed image quality.

V. REFERENCES

[1] Kumar SN , Lenin Fred A, and Muthukumar S, '' A voyage on medical image segmentation algorithms'', *biomedical research, Special Section: Computational Life Sciences and Smarter Technological Advancement*,2018

[2] Abdelaziz E, Elhoussaine O and Abdenbi B,'' Medical Image Segmentation by Active Contour Improvement '', *American Journal of Software Engineering and Applications*, 6, (2), 2017, pp. 13-17

[3] Sanping Z , Jinjun W, Shun Z, '' Active Contour Model Based on Local and Global Intensity Information for Medical Image Segmentation'', *Preprint submitted to Journal of Neurocomputing, september* 2016.

[4] Adegoke, B. O , Olawale, B. ., Olabisi, N.I, '' Overview of Medical Image Segmentation'', *International Journal of Engineering Research and Development*, 8, (9), September 2013

[5] M. Beladgham, A. Bessaid, A. Taleb-Ahmed and I. Boucli Hacene, "Medical Image Compression Using Quincunx Wavelets and SPIHT Coding", Journal of Electrical Engineering & Technology Vol. 7, No. 2, pp. 264~272, 2012

[6] Daniel J. Withey and Z.J. Koles, "A Review of Medical Image Segmentation: Methods and Available Software", International Journal of Bioelectromagnetism, Vol. 10, No.3, pp.125-148, 2008

[7] R. Loganathan and Y. Kumaraswamy, "Active contour based medical image segmentation and compression using biorthogonal wavelet and embedded zerotree," Indian Journal of Science and Technology, vol. 6, pp. 4390-4395, 2013.

[8] P.nagaswara Reddy and C.P.V.N.J Mohan Rao, "BRAIN MR IMAGE SEGMENTATION BY MODIFIED ACTIVE CONTOURS AND CONTOURLET TRANSFORM", ICTACT journal on image and video processing, vol.08, novembre 2017

[9] J. A. Sethian, level set Methods and Fast Marching Methods, second ed., Cambridge University Press, 1999.

[10] S. Osher and J. A. Sethian, "Fronts propagating with curvature dependent speed: algorithms based on Hamilton-Jacobi formulations," Journal of Computational Physics, vol. 79, no. 1, pp. 12– 49, 1988.

[11] T. Chan and L. Vese, "Active contours without edges," IEEE Trans. Image Process. 10, 266–277 2001.

ISSN 1737-930X

[12] M. Beladgham, F. Derraz, '' Segmentation d'images médicales IRM par la méthode d'ensembles de niveaux (Level_Sets)'', Abou- Bekr Belkaid university –Tlemcen, january,2005
[13] L. Tingting Xu. Haiyong Xu, "Medical Image Segmentation Based on a Hybrid Region-Based Active Contour Model", Hindawi Publishing Corporation,Computational and Mathematical Methods in Medicine, vol14, juin 2014
[14] Dimitri VD., Thierry B. and Michael U. "On the Multidimensional Extension of the Quincunx Subsampling Matrix'', IEEE Signal Processing Letters, Vol. 12, No. 2, FEBRUARY 2005.
[15] Chen Y. Michael AD. and Wu-Sheng L. "Design of Optimal Quincunx Filter Banks for Image Coding'', EURASIP Journal on Advances in Signal Processing, Vol. 2007.
[16] Lee L., Oppenheir V.A., "Proprerties of approximate parks-McClellan filters'', IEEE, pp.2165-2168; 1997;
[17] Miaou S.G., Chen S.T. and Chao S.N., "Waveletbased lossy-to-lossless medical image compression using dynamic VQ and SPIHTcoding'', Biomedical engineering-applications, basis & communications, Vol. 15 No3, p 235-242, December 2003.
[18] Said A. and Pearlman W. A., "A new fast and efficient image codec based on set partitioning in hierarchical trees'', IEEE Trans. Circuits and Systems for Video Technology, Vol. 6, p243 – 250, June 1996.
[19] Vetterli M. and Kovacevé J., "Wavelets and Subband Coding'', Upper Saddle River, NJ: Prentice-Hall, 1995.
[20] Manuela F., Dimitri VD. and Michael U., "An Orthogonal Family of Quincunx Wavelets With Continuously Adjustable Order'', IEEE Transactions On Image Processing, Vol. 14, No. 4, APRIL 2005
[21] Yen-Yu C. and Shen-Chuan T., "Embedded medical image compression Using DCT based subband decomposition and modified SPIHT data organization'', Proceedings of the Fourth IEEE, (BIBE'04), 2004.
[22] M. Beladgham , A. Bessaid,'' MRI IMAGE COMPRESSION USING
BIORTHOGONAL CDF WAVELET BASED ON LIFTING SCHEME AND SPIHT CODING'', Quatrième Conférence Internationale sur le Génie Electrique CIGE'10, 03-04 Novembre 2010, Université de Bechar, Algérie, Journal of Scientific Research vol. 2 (2010)
[23] Wang Z., Bovik A. C., Sheikh H. R. and Simoncelli E.P, "Image quality assessment: From error visibility to structural similarity'', IEEE Transactions on Image Processing, Vol. 13, No. 4, APRIL 2004.
[24] Wang Z. and Bovik A. C, "A universal image quality index'', IEEE Signal Processing Letters, Vol. 9, pp.81–84, Mar. 2002
[25] www.GE Medical System.com (database).

ISSN 1737-930X